Survey Review

ISSN: 0039-6265 (Print) 1752-2706 (Online) Journal homepage: https://www.tandfonline.com/loi/ysre20

LIDAR-based roadway and roadside modelling for sight distance studies

M. Castro, S. Lopez-Cuervo, M. Paréns-González & C. de Santos-Berbel

To cite this article: M. Castro, S. Lopez-Cuervo, M. Paréns-González & C. de Santos-Berbel (2016) LIDAR-based roadway and roadside modelling for sight distance studies, Survey Review, 48:350, 309-315, DOI: 10.1179/1752270615Y.0000000037

To link to this article: https://doi.org/10.1179/1752270615Y.0000000037

Published online: 11 Apr 2016.

LIDAR-based roadway and roadside modelling for sight distance studies

M. Castro*, S. Lopez-Cuervo, M. Paréns-González and C. de Santos-Berbel

Sight distance is a key aspect of road design and operation because of its relationship to traffic safety. The most realistic procedures for calculating the section of roadway visibility to the driver require the use of digital elevation models (DEM), which represent both the roadway itself and the features along the roadside. In this study, the influence of different types of DEM, an essential asset in sight distance analysis, is evaluated. Digital terrain models (DTMs), which represent the bare ground surface, and digital surface models (DSMs) that also consider elements above the terrain have been utilised. Both are high-resolution models obtained through airborne Light Detection and Ranging (LIDAR) or terrestrial vehicle (Mobile Mapping System, MMS). In addition, this study shows the influence of roadside vegetation on sight distance, revealing the underlying difficulties and suggesting possible solutions for sight distance studies when using these models.

Keywords: Digital elevation model, Road safety, Sight distance, GIS, Mobile mapping system, LIDAR

Introduction

Sight distance is a key element not only in road design but also in road management owing to its relationship to traffic safety. When a vehicle is travelling on the road, the section of roadway viewed by the driver (measured along the hypothetical path the vehicle is following) ought to be greater than the distance needed to perform emergency stops at any time. Available sight distance also plays an important role at intersections and for passing manoeuvres.

Several factors are involved in sight distance calculations: the height of the observer, the height of the target object on the roadway, the vehicle path and the shape of the terrain (meaning both the pavement surface itself as well as the roadsides). Traditionally, Digital Terrain Models (DTMs) have been utilised to determine available sight distances. Such elevation models represent the bare earth, so that elements such as bushes, trees or buildings are not considered. Nowadays, an increasing number of Digital Surface Models (DSMs) and field studies, which do consider vegetation and buildings are available for sight distance studies, thanks to the use of LIDAR (Light Detection and Ranging) technologies, either airborne or terrestrial (mounted on a vehicle).

An adequate representation of the terrain is essential to obtain a realistic sight distance outcome. Although at first approach, it may seem that DSMs are more appropriate for this task, their application is not without problems. The main aim of this paper is to analyse the influence of DTM and DSM features on the outcome of sight distance calculation in highways.

Technical University of Madrid, Spain

*Corresponding author, email maria.castro@upm.es

First, basic concepts for the study are reviewed, including available sight distance on highways, its calculation using Geographic Information Systems (GIS) and the different types of Digital Elevation Models (DEM), i.e. DTM and DSM. Next, the materials and methods utilised for the study are described: the highway studied, the characteristics of the DEMs, and the software and the approach used in the study. Moreover, a comparative study of the available sight distance along the whole highway section has been performed and three more detailed studies have been carried out afterwards, selecting three types of scenario with different vegetation densities.

Background

Available sight distance may be defined as the maximum section of roadway ahead that a driver can see without the line of sight being obstructed by any feature of the roadway itself or on the roadsides. Figure 1 shows the concept of available sight distance according to highway design guide standards. Let us consider a vehicle that will follow a trajectory (dotted line) along a horizontal curve where there is an obstacle (coloured brown in on-line version) to the right of the curve. When such a vehicle is placed at station A, lines AB, AC, ..., AJ are the lines of sight from the driver's eye. The driver sees both section AD and section HJ, although the obstacle prevents the driver from seeing section DG. In this case, available sight distance is defined as the arc distance AD. The importance of available sight distance can be observed, for instance, in this case by supposing an obstacle (i.e. a fallen tree, or a dead animal) is on the roadway at point D. The available sight distance at A (arc AD) should be greater than the distance required to stop the vehicle.

There are several methods or procedures to calculate sight distance (Larocca *et al.*, 2011). However, the use of a GIS in highway sight distance studies has several

Received 31 July 2014; accepted 14 May 2015
DOI 10.1179/1752270615Y.0000000037

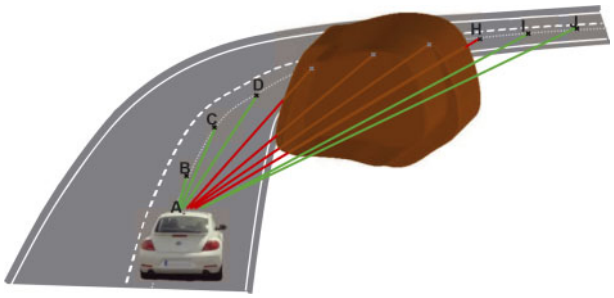

1 Lines of sight (segments AB, AC, ..., AJ) and available sight distance (length of arc AD)

advantages over the use of traditional road design software. It allows this analysis to be combined with other traffic safety studies, such as crash and design consistency. In this way, more comprehensive studies can be carried out and costs shared (Castro and De Santos-Berbel, 2015). It permits the analysis of available sight distance on existing highways where project data may not be either available or reliable. It allows the use of data sources that, besides the terrain itself, include obstacles such as trees or buildings that could reduce driver sight distance (Khattak and Shamayleh, 2005; Castro *et al.*, 2011; Castro *et al.*, 2014). Matos *et al.* (2014) researched the influence of median barriers on sight distance on dual-carriageways by means of three-dimensional simulations. For sight distance calculations both DEM (terrain or surface) and the vehicle path are needed.

A DEM is a 3D model representing a terrain's surface and, occasionally, other landscape features, through a collection of points or linear elements that shape terrain elevations. There are two types of DEM: DTM and DSM. A DTM is a DEM, which represents the bare ground surface. A DSM also considers objects existing on the surface; in other words, it depicts elements like trees, buildings, etc. Each DEM may depict the same terrain surface in two different ways depending on the surveying procedure and the data processing methods used.

In the case of road studies, surveying sensors that collect data for DEMs are usually airborne or mounted on a car. The latter constitute a Mobile Mapping System (MMS), also known as Mobile Terrestrial Laser Scanning (MTLS) (Caroti and Piemonte, 2010; Xiushan *et al.*, 2011; Gong *et al.*, 2012; Findley *et al.*, 2013; Puente *et al.*, 2013). This consists of an integrated system composed one or more LIDAR sensors combined with a position system and a photographic camera all on board the surveying vehicle. Such LIDAR devices, each installed in a known position of the vehicle, scan the ground surface (Moreno *et al.*, 2013) so that all sensors operate simultaneously. The three-dimensional (3-D) position data of the points reached by these lasers are stored along with 360° images taken at the position where the 3-D points were captured. The cloud of points obtained through laser scanning is very versatile since it provides 3-D coordinates of the points directly (Yoo *et al.*, 2010). This enables not only a more realistic 3-D visualisation of the entire route but also a significant reduction of time in data collection and data processing.

Materials and methods

The available sight distance has been studied along a road with many elements along its roadsides (mainly trees) that could reduce sight distance. Three different types of DEM have been used: DTM01, DSM01 and DSM MMS. DTM01 and DSM01 are high-resolution models obtained through airborne LIDAR (Fig. 2*a*). While DTM01 is a DTM, DSM01 is a DSM. The grid size of both models is small (1 m) so that these representations provide a close fit to the ground surface and the elements on it. The data acquisition for both elevation models comes from the same survey since this technology allows up to four signal returns per pulse. While the upper returns would correspond to the vegetation cover and other features, the lower ones would detect the soil. The scanning frequency of the airborne LIDAR sensor is 70 Hz and the minimum pulse frequency is 45 kHz, with a range of up to 3000 m. The flight for data acquisition was not specially programmed to survey the road but rather for general purposes (IGN, 2010). For this reason, the points on the grid are not aligned with the road (Fig. 2*a*).

The point cloud of the DSM MMS differs from the two models described above since it was obtained through a MMS. The IPS2-Compact equipment from Topcon comprises an odometer, an inertial measurement unit (IMU), GNSS antenna and receiver, IP-S2 box, 3 class 1 scanning lasers and a 2MPX 360° digital camera (Topcon, 2010). This equipment is able to capture 3-D point collections from the roadway and the elements along either roadside regardless of lighting conditions. Laser beams are mounted on the surveying car so that they span the roadway as well as most elements on the roadsides: two lasers are mounted to point sideward from the vehicle and a third laser points downward at the rear of the vehicle. The typical measurement accuracy of these laser scanners is ± 35 mm; their data update/output rate is 75 Hz; and their typical range is 30 m. The remaining components of the MMS equipment are used to locate and position the surveyed area. While the GNSS device sets the geospatial position, the IMU device records the orientation while the odometer measures the distance travelled and the speed. Vehicle speed during surveying was approximately 50 km h^{-1} so that points are arranged in 0.15-m spaced profiles along the highway centreline. Crosswise to the centreline, the points are arranged so that they are close together and spread out evenly when closer to the scanner, whereas the grid is more irregular and dispersed as the distance from the scanner increases.

Figure 2*a* shows the evenly distributed grid (1 m spaced) of models DTM01 and DSM01, which is not, however, aligned to the road centreline, as the surveying was conducted using a general purpose flight. In contrast, MMS survey points are arranged in a fairly regular layout around the road centreline where the longitudinal gap is almost constant (0.15 m) and the cross-distance is variable (Fig. 2*b*). Figure 3*a* shows how the surveying flight collects information about the elements of the ground surface (terrain, buildings, trees, etc.) as the plane moves forward. However, the data collected for DSM MMS are obtained from a vehicle that travels along the highway (Fig. 3*b*) and the survey is conducted using laser beams projected perpendicularly to the vehicle path.

Data handling performed with either model used in this study followed the same steps. First, a Triangulated Irregular Network (TIN) was created by the point cloud using

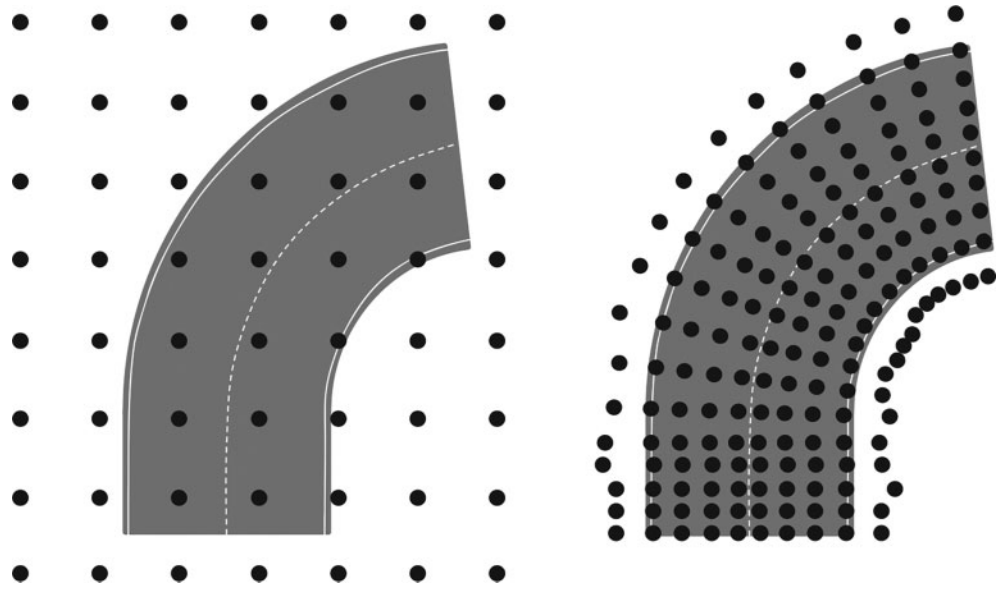

2 Point collection layout obtained from airborne light detection and ranging (LIDAR) *a* and terrestrial LIDAR [mobile mapping system, (MMS)] *b*

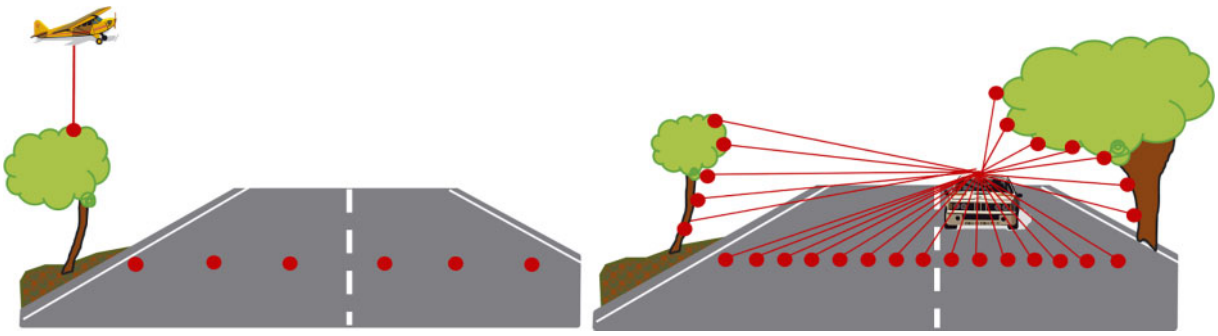

3 Surveying procedure from airborne light detection and ranging (LIDAR) *a* and terrestrial LIDAR [Mobile Mapping System (MMS)] *b*

ArcGIS tools according to Delaunay triangulation criteria. Next, available sight distance calculations were performed using specific software in the ArcGIS environment (Castro *et al.*, 2014). The height of the driver's eye above the pavement surface was taken to be 1.1 m, whereas the height of the target object on the roadway was taken to be 0.2 m in all cases, according to Spanish geometric design standards (Ministerio de Fomento, 2000). The height of the driver's eye (1.1 m) corresponds to the view from a passenger car. In addition, in order to determine the actual vehicle path, a real vehicle was used for the calculations. For this purpose, a car travelled (several times each way) along the highway studied. This car had a 10-Hz GNSS receiver installed on the roof above the driver's position (attached to a magnetic platform). The most complete trajectory dataset was chosen for each direction and this dataset was checked on the GIS. A 20-cm-pixel resolution orthophoto was inspected to check that the entire length of each path matched the centre of the corresponding lane. A polyline was made out of the points collected in each direction and, after that, a set of stations spaced 5 m apart was created. These polylines were utilised in the computation.

In essence, the application for available sight distance calculation launches a sight beam from every station on the vehicle path towards the stations ahead, determining whether the obstacle would be seen by the driver. This software then returns the distance between the position of the driver and the farthest target they would see measured along the vehicle path. The algorithm executes a loop starting at station A and successively launches a line-of-sight beam to stations B, C, ..., J (Fig. 1). As mentioned above, available sight distance is defined as the distance, measured along the vehicle path, between the starting station (A in Fig. 1) and the farthest target station seen without the line of sight being interrupted (station D in Fig. 1). Once the analysis from station A has been completed, the virtual driver is moved forward to station B, where an identical loop continues to launch a line-of-sight beam towards stations C, D, ..., J.

Once the outcome of the sight distance study had been obtained for the three cases (DTM01, DSM01, DSM MMS), the next step was to carry out a comparative analysis of the results. Both Kolmogorov–Smirnov and Mann–Whitney–Wilcoxon tests were applied to the outcome in order to determine whether it might be considered that the three series of results statistically come from the same distribution. Also, the Euclidean Distance (ED) between the resulting sight distance functions was calculated using sight distance in DTM01 as a base equation (1).

$$ED = \sqrt{\sum_{i=1}^{n} \frac{(y_{DSM,i} - y_{DTM,i})^2}{n}} \quad (1)$$

Where $y_{DTM,i}$ is the ith value of sight distance in DTM01, $y_{DSM,i}$ is the ith value of sight distance in DSM01 or in DSM MMS, as appropriate, and n is the sample size.

It has been observed that the major differences in sight distance between models correspond to areas where there are elements above the roadsides, mainly trees. In order to study the influence of such elements in greater detail, three possible scenarios were selected:

1. areas with sparse vegetation
2. slightly wooded areas
3. densely wooded areas (tree crowns hanging partially over the roadway).

Results and discussion

As mentioned previously, a Kolmogorov–Smirnov test was used to determine whether the three series (gross values) might come from the same distribution. This test was performed considering the three samples in pairs. For each of the three possible combinations, p-values were much less than 0.05, so there is a statistically significant difference between all the distributions at the 95.0% confidence level (Table 1).

Furthermore, a Mann–Whitney–Wilcoxon test was employed to compare the means of the three samples in pairs through a t-test. On this occasion, since p-values were again lower than 0.05, there is a statistically significant difference between the means of the two samples at the 95.0% confidence level. Finally, the ED [equation (1)] between sight distance functions was calculated in pairs, using the sight distance outcome obtained in DTM01 as a base. In the case of DSM01, the ED was 128.59 m, while in the case of DSM MMS it was 147.93 m (Table 2). Such values, although within the standard deviation of DTM01 (204.832 m), are quite significant in terms of required sight distance for manoeuvers such as emergency stops, passing or merging.

Therefore, according to the statistical study (Tables 1 and 2), the available sight distance obtained for each elevation model was significantly different. The main differences are in leafy areas. The results in the three scenarios studied are explained below more in detail.

Table 1 Outcome of the statistical study

	DTM01 versus DSM01	DTM01 versus DSM MMS	DSM01 versus DSM MMS
W	-1.23×10^6	-1.18×10^6	185 507
p-value	0.0000	0.0000	0.0056

Table 2 Statistical parameters of the samples

	DTM01	DSM01	DSM MMS
Count	2998	2998	2998
Average	253.26	189.59	180.36
Standard deviation	204.83	200.20	154.33
Coeff. of variation	80.88%	105.60%	85.57%
Minimum	5.0	0.0	0.0
Maximum	1000.0	1000.0	800.0
Range	995.0	1000.0	800.0
Euclidean distance (ED)	–	128.59	147.93

Scenario 1: areas with sparse vegetation

A section of road was chosen, from station 2600 to 2900. This section is surrounded mainly by low height crops and a few isolated trees. In the horizontal projection, the road is on a tangent.

Figure 4 shows the results obtained in this section. The horizontal axis represents stations along the trajectory, whereas the vertical axis represents available sight distance. The available sight distances obtained for each elevation model follow the same tendency, the differences being smaller than 10 m at any station within this section. This fact supports the hypothesis that, in the absence of dense vegetation or other elements by the roadsides, the available sight distance outcome for all elevation models is very similar. Slight differences between models DTM01 and DSM01, if any, may be caused by sparse vegetation. Small differences between DTM01 and DSM MMS might be produced by differences in resolution and model structure.

Scenario 2: slightly wooded area

A section of road was chosen, which had a substantial number of trees on either side, but the tree crowns did not overhang the roadway. The section runs from station 8450 to 8700.

Available sight distance obtained using DTM01 is greater than the outcome using the DSMs (Fig. 5). The differences in sight distance values between model DTM01 and each of the DSMs are approximately 70 m in this section. However, available sight distances for the two DSMs are very similar, differing by 5 m or less. These results were foreseeable and confirm the influence of vegetation in available sight distance. In sections where elements by the roadsides (such as shrubbery or trees) are not considered by the DTM, the available sight distance obtained using a DSM will be shorter. Small differences between sight distances using the DSMs may be caused by differences in grid resolution between the two models and their varying adaptation to the environment.

Scenario 3: densely wooded areas (tree crowns hang partially over the roadway)

A section of road, from station 4350 to 4590, was selected that had large trees on the roadsides with some of their crowns overhanging the roadway; in other words, the tree crowns formed a canopy over the pavement surface.

Figure 6 shows the different results obtained using the elevation models proposed. Similar to scenario 2, available sight distances for DTM01 are equal to or greater than those for the DSMs. In contrast to the results for scenario 2, significant differences in sight distance values between the two DSMs were also found. In this case, they were actually greater than 100 m. In addition, this chart highlights the fact that the study using DSM01 produces an outcome that is significantly different from the other two, especially around station 4575 where sight distance is supposed to be null.

The MMS takes 360° images of the environment along the path travelled by the surveying vehicle. Such snapshots also contain information of the position where they were taken. A detailed visual inspection was also performed on the spot, and the whole highway section was filmed from the moving vehicle. The researchers could, therefore, check the real visibility

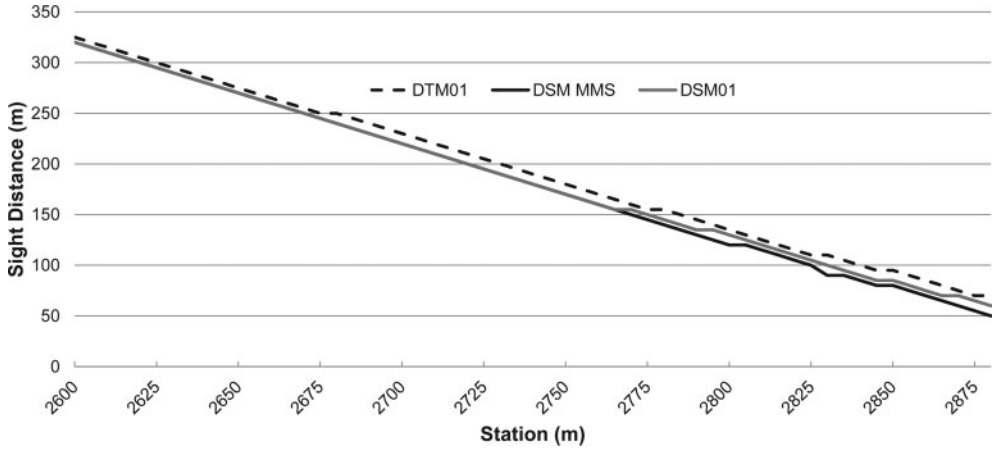

4 Sight distance results in areas with sparse vegetation (scenario 1)

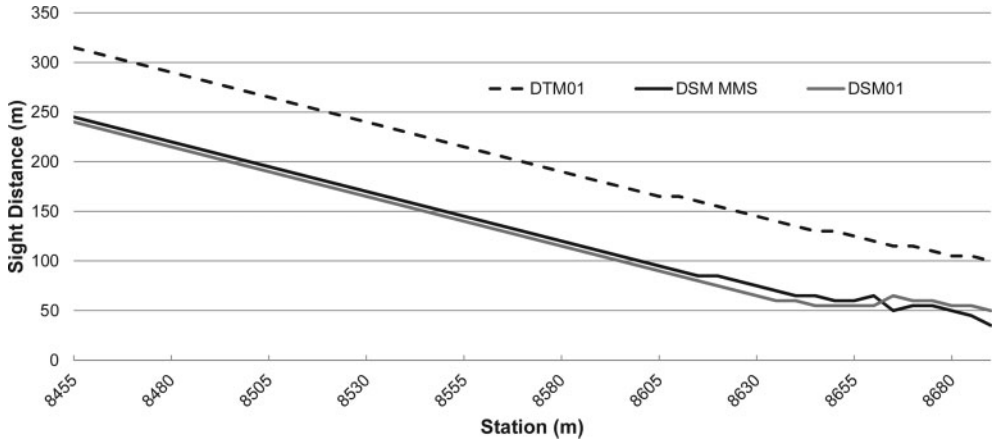

5 Sight distance results in slightly wooded areas (scenario 2)

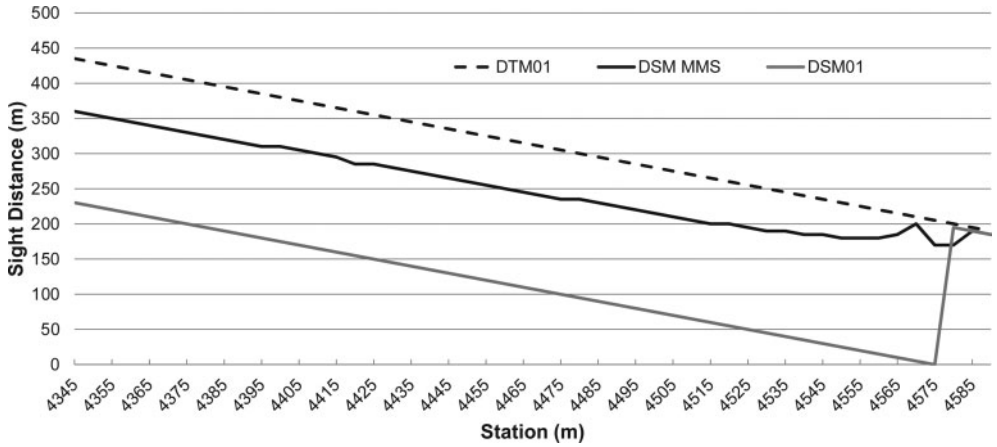

6 Sight distance results in densely wooded areas with tree crowns partially over the roadway (scenario 3)

conditions by the roadside in those cases where the sight distance outcome did not seem realistic. After checking, it was concluded that the vegetation around station 4575 is not so dense as to completely block the visibility of the road to the driver. Thus DSM01 did not properly depict the real scene in that section.

Figure 7 represents a plane view of the TIN created for each elevation model along with the vehicle path, once discretised, as well as the markings of the roadway edges. The selection includes the section from station 4565 to 4585. Around station 4575, there is a tree close to the roadside. The TIN of DSM01 (Fig. 7*b*) shows an obstacle that spans the whole lane at the top, which is the tree located close to the roadside. This tree can also be discerned in the TIN of DSM MMS (Fig. 7*c*), yet the overhang above the roadway is not as wide as for DSM01. This discrepancy is due to the higher resolution of DSM MMS, which enables the model to better fit the shape of the trees. As expected, the TIN of DTM01 (Fig. 7*a*) did not represent this obstacle, which is not part of the ground surface.

The explanation of why DSM01 did not accurately depict the actual shape of the tree crown above the

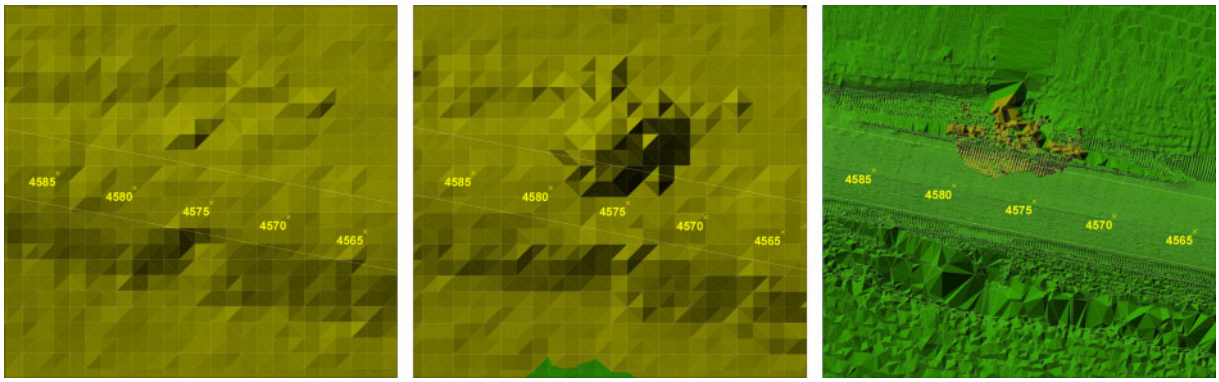

7 Different triangulated irregular network (TIN) models of the same section: *a* DTM01; *b* DSM01; *c* digital surface model (DSM) mobile mapping system (MMS)

roadway lies in the Delaunay triangulation procedure used to create the TIN surface. The intrinsic definition of a Delaunay triangulation impedes the overlapping of elements in the plane, i.e. the triangles created are arranged in such a way that they can only connect points whose distance in the plane is minimum, even if there are closer points from a 3-D approach. For this reason, Delaunay triangulation connects points in the tree crown with points on the pavement surface, creating a sort of wall that does not actually exist.

In those cases where the vertical crown projection of large trees on the roadsides lies on the roadway, previous data processing would be desirable in order to prevent incorrect results. All surveyed points lying above the roadway should be eliminated or, at least, their height should be modified. Nonetheless, if some of the surveyed points are removed, the grid could lose its homogeneity and accuracy and the TIN might be distorted. Removing height information creates empty areas, which is more troublesome in the case of DSM01, where the grid size is far greater than for DSM MMS. Modifying the height of the points where the tree crown overhangs the roadway is an alternative method. It consists of seeking points with heights that indicate that they are above the roadway and then shifting their height attribute to the height they would have if they were on the roadway. A drawback of this procedure lies in the fact that the height of the roadway is initially unknown, and so it has to be estimated through interpolation using nearby points on the roadway.

Whether point removal or height modification is chosen, the first step is to define the area to be altered. To carry out this task, lateral boundaries must be fixed following outer roadway markings (Fig. 8). Both procedures result in a clear section above the pavement, but taking roadside obstacles into consideration. In this way, the Delaunay triangulation preserves elements by the roadsides when creating a TIN, yet prevents calculation based on non-existent hindrances, thus avoiding systematic errors.

In this research, we opted to modify the value of the point height attribute. The height attribute of points within the boundaries of the roadway whose value was higher than they would have been if they were on the pavement surface was changed, and an interpolated value was assigned instead, using the height of nearby points on the roadway. The results obtained after performing this correction are shown in Fig. 9. Before the correction was made, available sight distance at station 4575 (Fig. 6) was null using DSM01, owing to the existence of a tree whose crown is partially above the roadway, whereas available sight distance was 200 m after the correction, resulting in a similar outcome for the three models employed.

Conclusions

In sight distance studies of roads where it is essential to take into account obstacles by the roadsides (such as trees or buildings), the use of a DSM is necessary if realistic results are to be achieved. To perform this task, high-resolution surface models obtained through LIDAR technology are required. Two procedures are available to obtain the DSM: either an airborne LIDAR survey or a MMS. Digital surface models obtained from surveying flights are more affordable since these may have been produced previously for some other purpose, while terrestrial surveying requires deploying a specially equipped vehicle to survey the road. However, a terrestrial MMS provides a greater density of points surveyed; hence the resulting surface model depicts the roadway and its roadsides more accurately. Additionally, the points on the grid obtained through the MMS are aligned with the road centreline, a feature that facilitates a better representation of the ground surface and the elements on it.

The resolution of DSM01 is constant (1-m spaced grid in this study), resulting in a more regular grid. By contrast, the resolution obtained through terrestrial MMS is variable, diminishing and becoming more irregular as the surveyed points are further from the scanner. Nonetheless, in sight distance studies both the resolution and the area covered by MMSs have proven to be sufficient.

There are some disadvantages when using a DSM to analyse sight distance, especially where elements by the roadsides overlap the roadway plane. The model incorrectly represents these areas because of the intrinsic definition of Delaunay triangulations: the algorithm employed to create a TIN does not allow overlapping elements on the plane. It was shown that trees whose crowns partially cover the roadside in the horizontal projection prevent the model from performing an accurate and realistic representation of the road. Hence the model shows an available sight distance equal to zero at nearby stations in the vehicle path, which is untrue. This issue is even more acute if an aerial DSM is utilised as an alternative to DSM MMS. To deal with these problems, data processing is needed in the areas affected by such overhanging elements, where either eliminating points or modifying their elevation may be suitable options. If the DSM comes from an aerial survey, it is advisable to modify the value of the elevation attribute to an interpolated

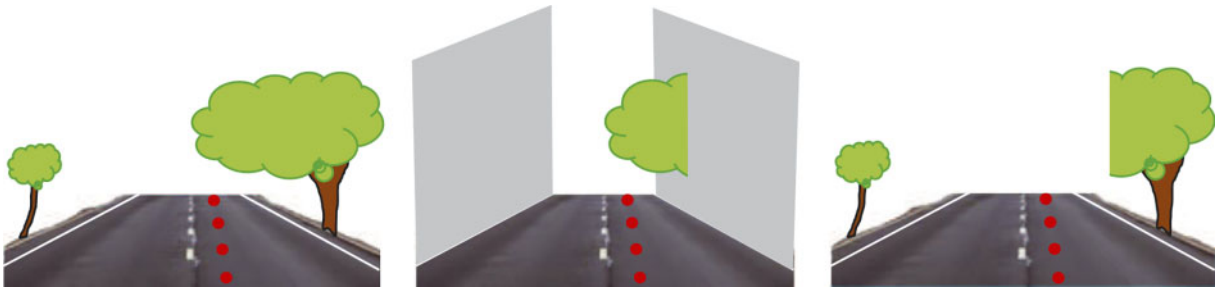

8 Selection of points to be modified or deleted above the pavement surface

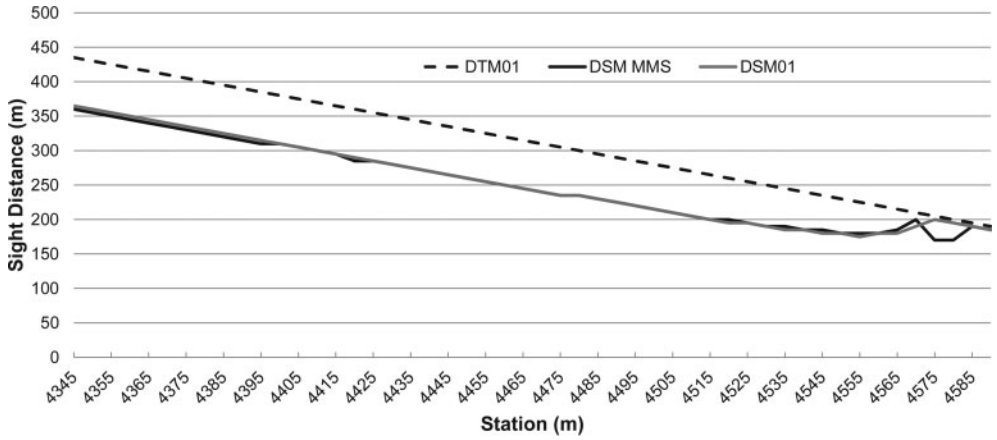

9 Sight distance results in a leafy section where a tree crown is partially over the roadway, after the correction is made to DSM01

value using nearby points on the pavement surface. Otherwise, if a DSM MMS is employed, awkward points in the cloud belonging to features over the roadway surface could be deleted without causing significant distortions, thanks to the high point density of these models.

Acknowledgements

The authors gratefully acknowledge the financial support of the Ministerio de Economía y Competitividad in research project TRA2011-25479 (Convocatoria de 2011 de Proyectos de Investigación Fundamental no Orientada del Plan Nacional de I + D + i 2008-2011).

References

Caroti, G. and Piemonte, A. 2010. Measurement of cross-slope of roads: evaluations, algorithms and accuracy analysis. *Survey Review*, 42(315), pp.92–104.

Castro, M. and De Santos-Berbel, C. 2015. Spatial analysis of geometric design consistency and road sight distance. *International Journal of Geographical Information Science*, DOI:10.1080/13658816.2015.1037304.

Castro, M., Anta, J. A., Iglesias, L. and Sánchez, J. A. 2014. GIS-based system for sight distance analysis of highways. *Journal of Computing in Civil Engineering*, 28(3), p.04014005.

Castro, M., Iglesias, L., Sánchez, J. A. and Ambrosio, L. 2011. Sight distance analysis of highways using GIS tools. *Transportation Research Part C Emerging Technologies*, 19(6), pp.997–1005.

Findley, D. J., Hummer, J. E., Rasdorf, W. and Laton, B. T. 2013. Collecting horizontal curve data: mobile asset vehicles and other techniques. *Journal of Infrastructure Systems*, 19(1), pp.74–84.

Gong, J., Zhou, H., Gordon, C. and Jalayer, M. 2012. Mobile terrestrial laser scanning for highway inventory data collection. In *Proceedings International Conference on Comp. in Civil Eng.*, American Society of Civil Engineers (ASCE), Clearwater Beach, FL, pp.545–52.

IGN. 2010. *LIDAR data sheet 606 of PNOA-LIDAR*. Madrid: Instituto Geográfico Nacional de España.

Khattak, A. J. and Shamayleh, H. 2005. Highway safety assessment through geographic information system-based data visualization. *Journal of Computing in Civil Engineering*, 19(4), pp.407–11.

Larocca, A. P. C., da Cruz Figueira, A., Quintanilha, J. A. and Kabbach Jr., F. I. 2011. First steps towards the evaluation of the efficiency of three-dimensional visualization tools for detecting shortcomings in alignment's coordination. In *Proceedings 3rd International Conference on Road Safety and Simulation*, Transportation Research Board, Indianapolis, IN.

Matos, E. S., Larocca, A. P. C. and Kabbach Jr, F. I. 2014. Study of the position of barrier lines on two-way highways by three-dimensional simulations. *Engineering Science Letters*, 1, pp.1–18.

Ministerio de Fomento. 2000. *Norma 3.1-IC Trazado*. Madrid: Ministerio de Fomento.

Moreno, F. A., González-Jiménez, J., Blanco, J. L. and Esteban, A. 2013. An instrumented vehicle for efficient and accurate 3D mapping of roads. *Computer-Aided Civil and Infrastructure Engineering*, 28(6), pp.403–19.

Puente, H., González-Jorge, H., Martínez-Sánchez, J. and Arias, P. 2013. Review of mobile mapping and surveying technologies. *Measurement*, 46, pp.2127–45.

Topcon. 2010. *IP-S2 specifications*., Available at: <http://www.topcon.co.jp/en/positioning/products/pdf/ip_s2.pdf> [Accessed 19 January 2013]

Xiushan, L., Bo, S. and Dong, W. 2011. 3DSurs - an example of the development of mobile mapping systems in China. *Survey Review*, 43(322), pp.415–26.

Yoo, H. J., Goulette, F., Senpauroca, J. and Lepère, G. 2010. Analysis and improvement of laser terrestrial mobile mapping systems configurations. *International Archives of Photogrammetry, Remote Sensing and Spatial Information Science*, American Society of Civil Engineers (ASCE), Newcastle Upon Tyne, UK, Volume 38 pp.633–8.